Supporting Information

Spermine-Responsive Supramolecular Chemotherapy System Con-structed from Water-Soluble Pillar[5]arene and Diphenylanthra-cene -Containing Amphiphile for Precise Chemotherapy

Yongfei Yin,†[a] Pei Zeng,†[b] Yifan Duan,[b] Jun Wang,[b] Wei Zhou,[c] Penghao Sun,[a] Zhanting Li,[c] Lu Wang,*[a]

Huageng Liang*[b] and Shigui Chen*[a]

[a] The Institute for Advanced Studies, Hubei Key Lab on Organic and Polymeric Opto-Electronic Materials, Wuhan University, 299 Bayi Road, Wuhan, Hubei 430072, China.

[b] Department of Urology, Union Hospital, Tongji Medical College, Huazhong University of Science and Technology, Jiefang Road 1277, Wuhan, Hubei 430022, China.

[c]Department of Chemistry, Department of Chemistry, Fudan University, 220 Handan Road, Shanghai 200433, China.

Email: sgchen@whu.edu.cn (Shigui Chen), leonard19800318@hust.edu.cn (Huageng Liang), wanglu-027@whu.edu.cn (Lu Wang)

Table of Contents

1 General information

Materials and Methods:

Materials: All reagents were purchased commercially and used without further purification unless otherwise noted. Minimum Eagle's medium (MEM) and Dulbecco's modified Eagle medium (DMEM) were purchased from Gibco (Thermo Fisher Scientific). Fetal bovine serum (FBS), penicillin-streptomycin and PBS were purchased from Invitrogen (Carlsbad, CA, USA). The Cell Counting Kit-8 (CCK-8) and 4',6-diamidino-2-phenylindole (DAPI) solution were purchased from Dojindo China Co. Ltd. (Shanghai, China).

Methods: UV-vis spectra were performed on a Pu xi TU-1900 spectrophotometer with 1 cm quartz cells. Fluorescence spectroscopic studies were carried out using a Ling guang F97 pro fluorescence spectrophotometer. ^{1}H NMR spectra, ^{13}C NMR spectra, and 2D NOESY NMR spectra were collected on a Bruker AVANCEIII 600 MHz instrument at 298 K. Chemical shifts are expressed in parts per million (δ) using residual solvent protons as internal standard. The couple constants values (J) are in Hertz (Hz). The following abbreviations were used for signal multiplicities: s, singlet; d, doublet; t, triplet; m, multiplet; and br, broad. Mass spectra were measured on a Bruker Daltonics Autoflex Speed Series: High-Performance MALDI-TOF Systems. DLS data were obtained on a Malvern Zetasizer Nano ZEN 3690. Transmission electron microscopy (TEM) images were recorded using field emission TEM (FE-TEM, F200). Confocal laser scanning microscope (CLSM) images were performed on Leica SP8 confocal laser scanning microscope. Flow cytometry analyses were conducted on a Beckman DxFLEX Flow Sight Imaging Flow Cytometer.

2. Synthetic Procedures

Compound **Gm**[1], **WP5C2**[2], and **WP5C5**[3] were synthesized following already reported protocol (Scheme S1-3).

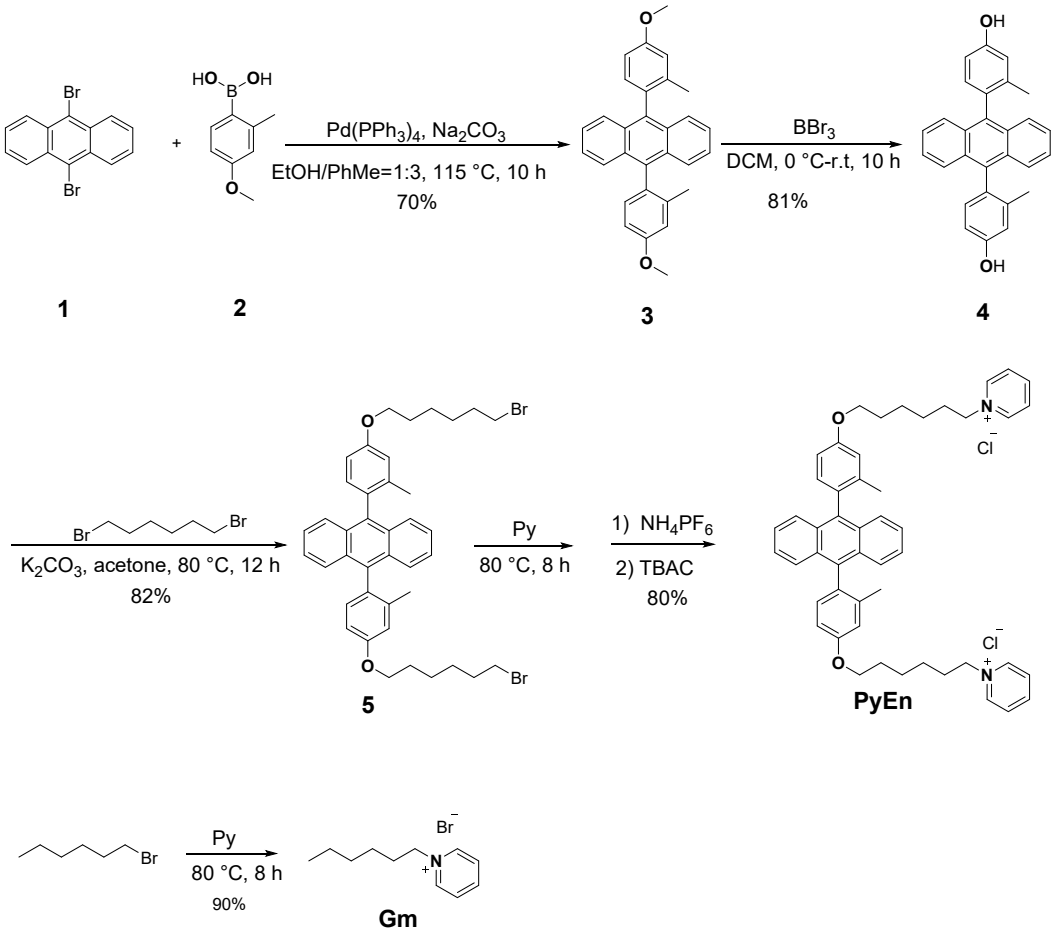

Scheme S1. The synthetic routes of compounds **PyEn** and **Gm**.

Compound 3. The compound 9,10-Dibromoanthracene (**1**) (1.00 g, 2.99 mmol), 4-methoxy-2-methylphenyl boronic acid (**2**) (1.00 g, 6.02 mmol), $Pd(PPh_3)_4$ (0.702 g, 0.608 mmol), Na_2CO_3 aqueous solution (10 mL, 2 mol/L), and 40 mL mixed solvent (ethanol/toluene = 1/3) were stirred and refluxed for 10 h under nitrogen. After the reaction finished, cooling down, and filtrated, the filtrate was collected and evaporated to remove the solvent. The resulting faint yellow solid was dissolved in dichloromethane (80 mL), after washing with water (3 × 60 mL) and brine (30 mL) and dried over anhydrous $MgSO_4$, the desiccant and solvent were removed by filtration and evaporation under reduced pressure in succession. The residue was further purified by

flash column chromatography using a binary solvent of dichloromethane/petroleum ether = 1:1 as eluent, compound **3** was isolated as faint yellow solid (0.887 g, 70%). ^{1}H NMR (600 MHz, $CDCl_3$, 298 K) δ (ppm): 7.60 (dd, *J* = 6.8, 3.3 Hz, 4H), 7.32 (dd, *J* = 6.8, 3.2 Hz, 4H), 7.23 (t, *J* = 7.9 Hz, 2H), 7.02 (d, *J* = 2.7 Hz, 2H), 6.96 (dd, *J* = 8.2, 2.7 Hz, 2H), 3.95 (s, 6H), 1.90 (s, 6H). ^{13}C NMR (150 MHz, $CDCl_3$, 298 K) δ (ppm): 158.1, 138.2, 134.9, 131.2, 129.6, 129.1, 125.8, 123.9, 114.4, 110.1, 54.2, 19.1. HRMS (ESI): Calcd for $C_{26}H_{27}O_2^+$ $[M+H]^+$: 419.2006. Found: 419.1993.

Compound 4. The compound **3** (0.780 g, 1.86 mmol) was dissolved in anhydrous dichloromethane (30 mL) under nitrogen, to which BBr_3 (0.5 mL) was dropwise added at ice bath. Then, the ice bath was removed and the reaction mixture was stirred at room temperature for 10 h, H_2O (20 mL) was dropwise added after TLC indicating the reaction was completed, the mixture was further filtered and washed with methanol (30 mL), The filter cake was evaporated under reduced pressure to discard the solvent, and compound **4** was obtained as faint yellow solid (0.587 g, 81%). ^{1}H NMR (600 MHz, DMSO-d_6, 298 K) δ (ppm): 9.57 (s, 2H), 7.50 (dt, *J* = 6.8, 2.8 Hz, 4H), 7.38 (ddt, *J* = 7.0, 3.4, 1.3 Hz, 4H), 7.05 (d, *J* = 8.1 Hz, 2H), 6.91 (d, *J* = 2.5 Hz, 2H), 6.83 (ddd, *J* = 7.8, 4.5, 2.5 Hz, 2H), 1.72 (d, *J* = 8.4 Hz, 6H). ^{13}C NMR (150 MHz, DMSO-d_6, 298 K) δ (ppm): 157.5, 138.6, 138.6, 136.2, 136.2, 132.4, 132.2, 130.1, 128.4, 128.4, 126.9, 126.8, 125.8, 117.2, 113.6, 20.2, 19.9. HRMS (ESI): Calcd for $C_{28}H_{22}O_2$ [M]: 390.1614 Found: 390.1607.

Compound 5. Compound **4** (300 mg, 0.769 mmol) and 1 ,6-dibromohexane (1.86 g, 7.69 mmol) were dissolved in 30 mL acetone, after the addition of K_2CO_3 (1.06 g, 7.69 mmol), the resulting suspension was refluxed for 12 h. Cooling down to room temperature when TLC indicated the reaction was completed. The organic solvent was removed by evaporating under vacuum, the remaining solid residue was further dissolved in dichloromethane (80 mL) and washed with H_2O (3 × 60 mL) and brine (30 mL), then dried over anhydrous $MgSO_4$. After removing the desiccant, the organic filtrate was concentrated by evaporation under reduced pressure and the residue was washed with petroleum ether. After drying under vacuum, Compound **5** could be

obtained (0.450 g, 82%) as white solid. ^{1}H NMR (600 MHz, $CDCl_3$, 298 K) δ (ppm): 7.59 (dd, *J* = 6.8, 3.3 Hz, 4H), 7.32 (dd, *J* = 6.8, 3.2 Hz, 4H), 7.21 (t, *J* = 8.4 Hz, 2H), 7.00 (d, *J* = 2.5 Hz, 2H), 6.94 (dd, *J* = 8.2, 2.6 Hz, 2H), 4.11 (t, *J* = 6.3 Hz, 4H), 3.48 (t, *J* = 6.8 Hz, 4H), 1.99-1.93 (m, 4H), 1.89 (s, 10H), 1.63-1.58 (m, 8H). ^{13}C NMR (150 MHz, $CDCl_3$, 298 K) δ (ppm): 158.7, 139.4, 136.1, 132.3, 130.6, 130.2, 126.9, 125.1, 116.0, 111.6, 111.6, 67.7, 34.0, 32.8, 29.3, 28.1, 25.5, 20.3. HRMS (TOF): Calcd for $C_{40}H_{46}Br_2O_2^{2+}$ $[M+2H]^{2+}$: 716.1865. Found: 716.1682.

Compound PyEn. Compound **5** (300 mg, 0.420 mmol) was dissolved in pyridine (5 mL), the resulting mixture was heated at 80 °C with stirring for 8 h until TLC suggested the completion of the reaction. Cooling down and removing the solvent by evaporation under reduced pressure. The remaining solid residue was then washed with ethyl acetate. The isolated pale yellow solid was dissolved in H_2O (5 mL), to which the saturated NH_4PF_6 aqueous solution was then added dropwise to generate pale yellow precipitates, which were collected by filtration and washed by another 20 mL of H_2O. The isolated pale yellow solid was dissolved in methanol (5 mL), to which excess tetrabutylammonium chloride was then added to generate pale yellow precipitates, which were collected by filtration and washed with another 20 mL of ethyl acetate. After drying under vacuum, compound **PyEn** could be obtained as pale yellow solid (0.264 g, 80%). ^{1}H NMR (600 MHz, MeOD, 298 K) δ (ppm): 9.08-9.05 (m, 4H), 8.66-8.60 (m, 2H), 8.15 (t, *J* = 7.0 Hz, 4H), 7.53 (dp, *J* = 7.5, 2.2 Hz, 4H), 7.36-7.30 (m, 4H), 7.16 (dd, *J* = 13.3, 8.3 Hz, 2H), 7.04 (d, *J* = 2.6 Hz, 2H), 6.98 (dd, *J* = 8.3, 2.7 Hz, 2H), 4.71 (t, *J* = 7.6 Hz, 4H), 4.14 (t, *J* = 6.2 Hz, 4H), 2.14 (p, *J* = 7.6 Hz, 4H), 1.91 (dt, *J* = 12.4, 6.4 Hz, 4H), 1.83 (d, *J* = 2.3 Hz, 6H), 1.72-1.65 (m, 4H), 1.56 (tt, *J* = 9.7, 6.2 Hz, 4H). ^{13}C NMR (150 MHz, $CDCl_3$, 298 K) δ (ppm): 158.9, 145.5, 144.6, 138.8, 135.9, 131.9, 130.3, 130.1, 128.2, 126.3, 124.9, 115.7, 111.6, 67.4, 61.7, 31.1, 28.8, 25.6, 25.4, 18.9, 18.8. MS (ESI) Calcd. for $C_{50}H_{54}N_2O_2^{2+}$ $[M-2Cl]^{2+}$, 357.2087, Found: 357.2078.

Compound Gm. 1-bromo-hexane (500 mg, 3.03 mmol) was dissolved in 5 mL pyridine, the resulting mixture was heated at 80 °C with stirring for 8 h until TLC suggested the completion of the reaction. Cooling down and removing the solvent by

evaporation under reduced pressure, the resulting pale yellow oil was washed with ethyl acetate. After drying under vacuum, compound **Gm** could be obtained as colorless oil (0.670 g, 90%). ^{1}H NMR (600 MHz, D_2O, 298 K) δ (ppm): δ 8.83 (d, *J* = 6.0 Hz, 2H), 8.53 (dd, *J* = 8.5, 7.1 Hz, 1H), 8.05 (t, *J* = 7.1 Hz, 2H), 4.60 (t, *J* = 7.3 Hz, 2H), 2.05-1.96 (m, 2H), 1.38-1.19 (m, 6H), 0.88-0.79 (m, 3H).^{13}C NMR (150 MHz, $CDCl_3$, 298 K) δ (ppm):145.5, 144.2, 128.2, 62.0, 30.5, 30.3, 24.8, 21.7, 13.2.

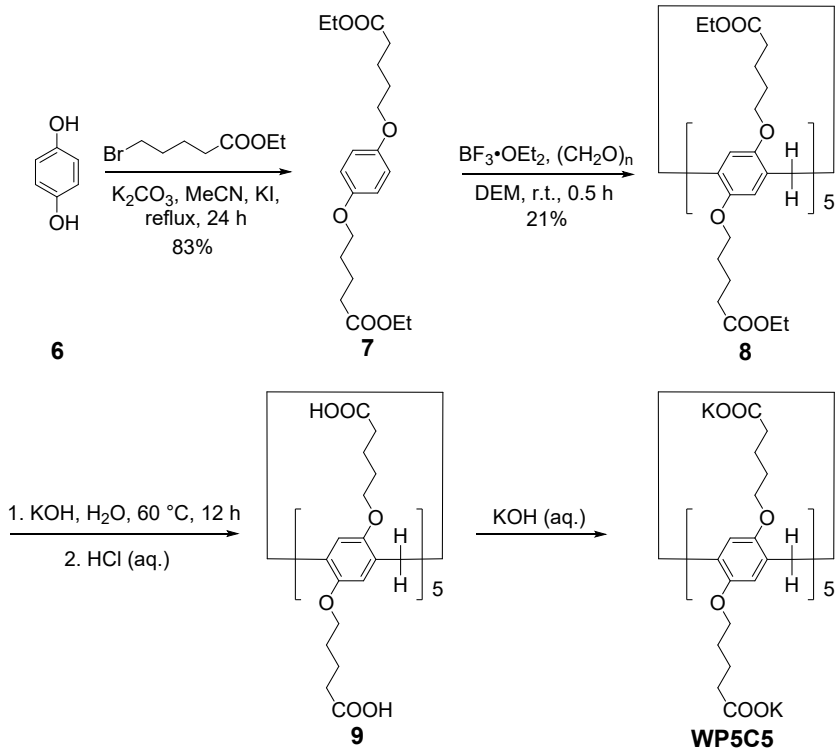

Scheme S2. The synthetic rout of compound **WP5C5**.

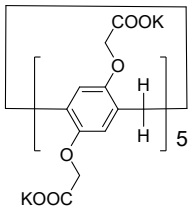

Scheme S3. The chemical structure of **WP5C2**.

3.Supporting Results and Experimental Raw Data.

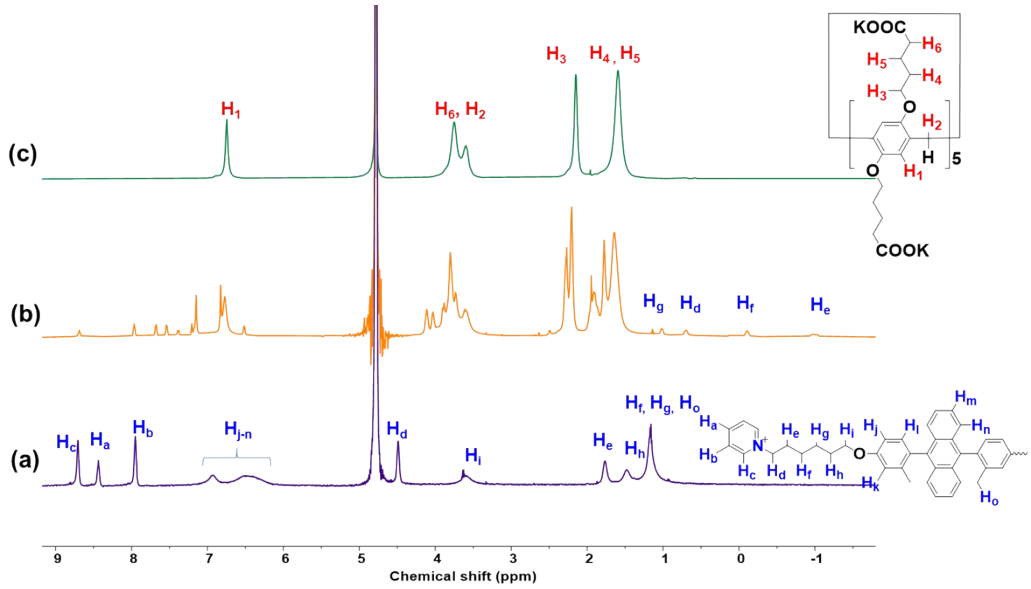

Figure S1.[1]H NMR spectra (600 MHz, D_2O, 298 K): (a) **PyEn** (5.0 mM); (b) mixture solution of **PyEn** (5.0 mM) and **WP5C5** (10.0 mM); (c) **WP5C5** (10.0 mM).

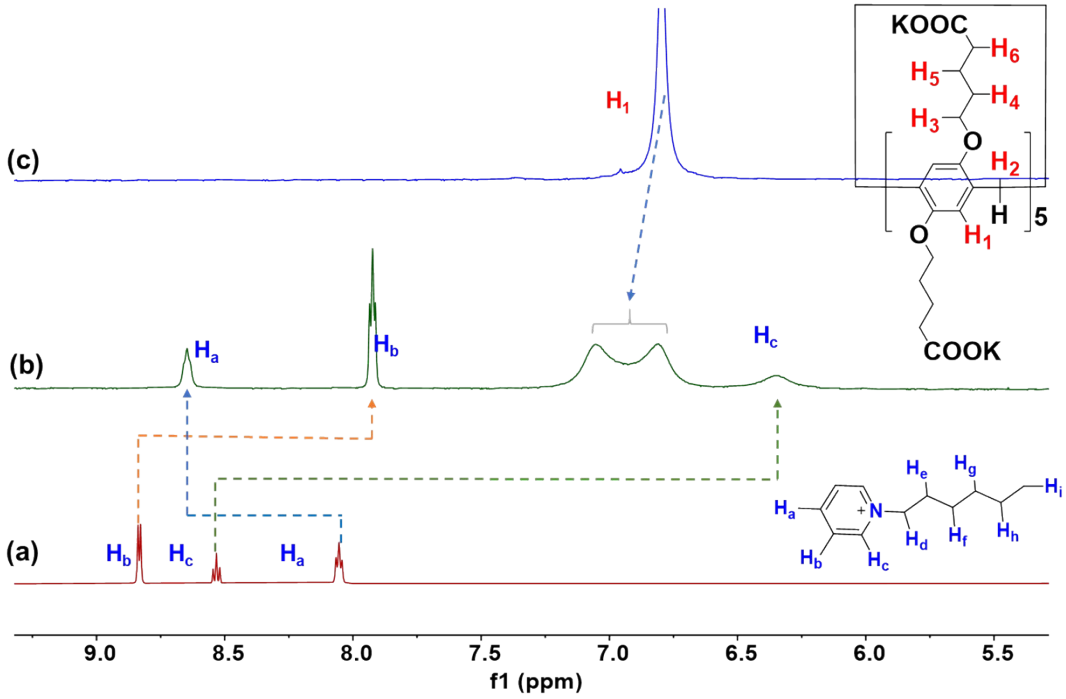

Figure S2. Partial [1]H NMR spectra (600 MHz, D_2O, 298 K): (a) **Gm** (5.0 mM); (b) mixture solution of **Gm** (5.0 mM) and **WP5C5** (10.0 mM); (c) **WP5C5** (10.0 mM).

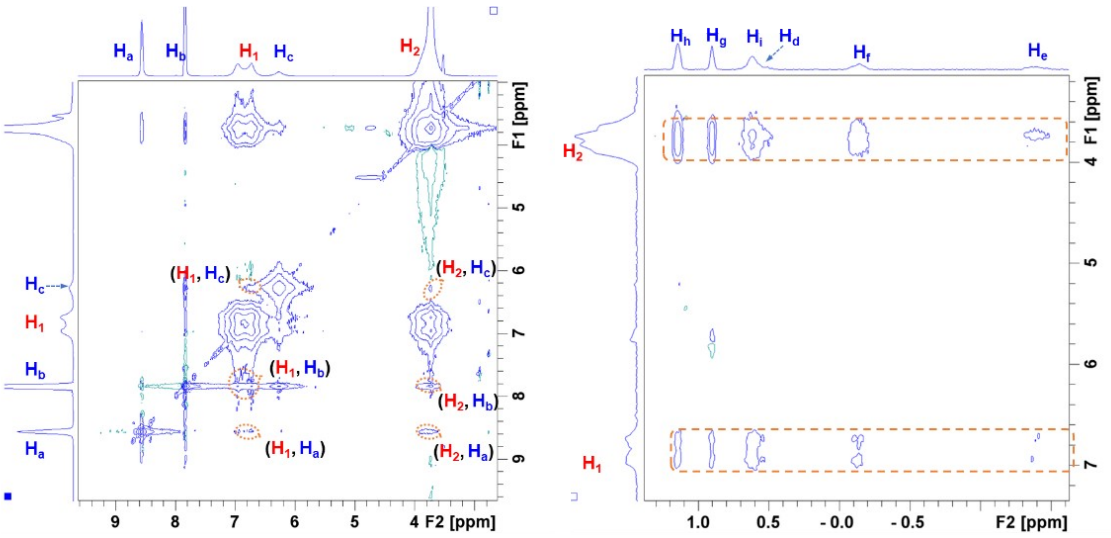

Figure S3. Partial 2D NOESY NMR spectrum (600 MHz, D_2O, 298 K) of **Gm** and **WP5C5** mixture at the ratio of 1:1. ([**Gm**] = 5 mM, [**WP5C5**] = 5 mM).

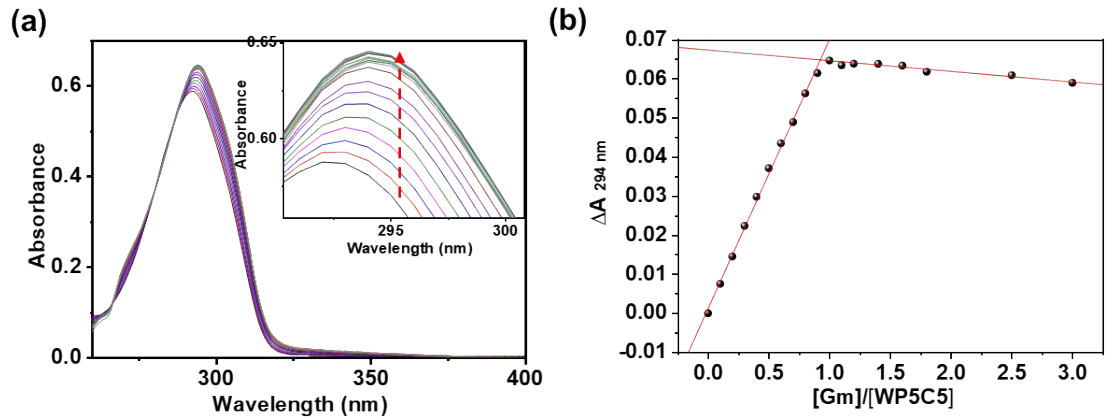

Figure S4. (a) UV-vis absorption spectra of the mixture of **WP5C5** and **Gm** in aqueous solution at different molar ratio. (b) Plot showing the 1:1 stoichiometry of the complex between **WP5C5** and **Gm** by plotting the difference in absorption at 294 nm (a characteristic absorption peak of **WP5C5**) against the molar fraction of **Gm** at an invariant total concentration of 0.033 mM in aqueous solution.

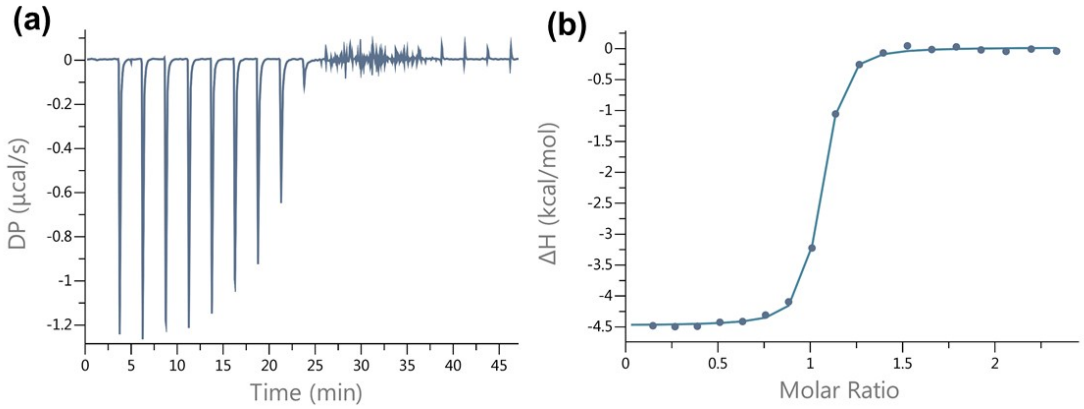

Figure S5. (a) Plot of DP vs time from the titration of host **WP5C5** (0.1 mM) and with guest **Gm** (1.00 mM) in H_2O; (b) plot of ΔH as a function of molar ratio. The solid line represents the best non-linear fit of the data to a 1:1 binding model (K_{app} = 4.05 × 10^6 M^{-1}, ΔH = -4.49 ± 0.027 kcal/mol, ΔG = -9.02 kcal/mol).

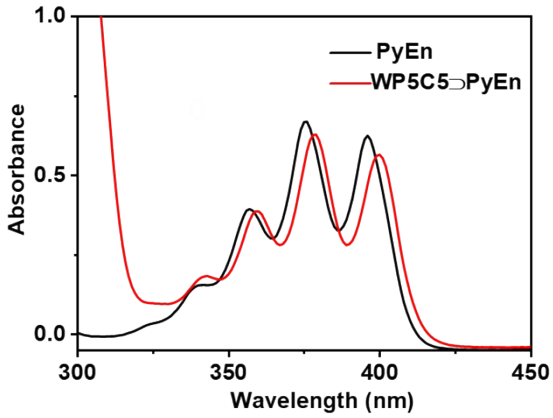

Figure S6. UV-vis spectra of **PyEn** (black line) and **WP5C5⊃PyEn** (red line).

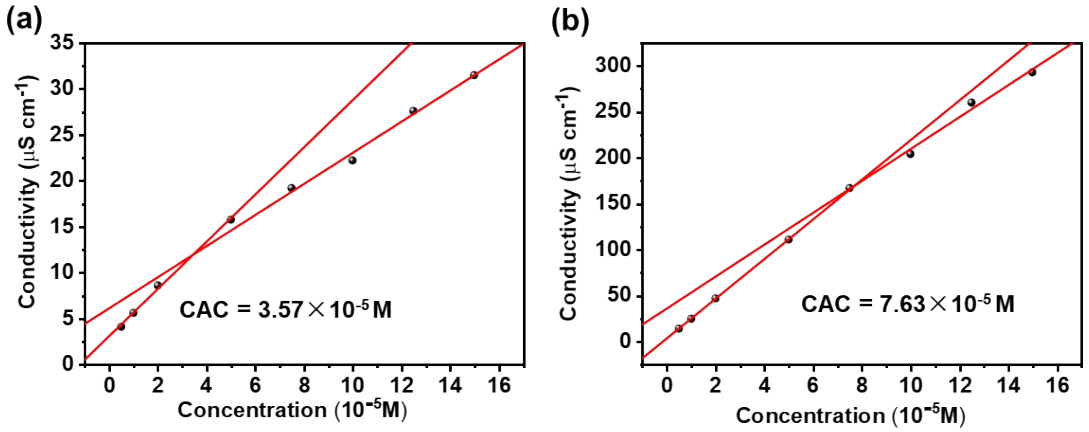

Figure S7. The concentration-dependent conductivity of (a) **PyEn** and (b) **WP5C5⊃PyEn**.

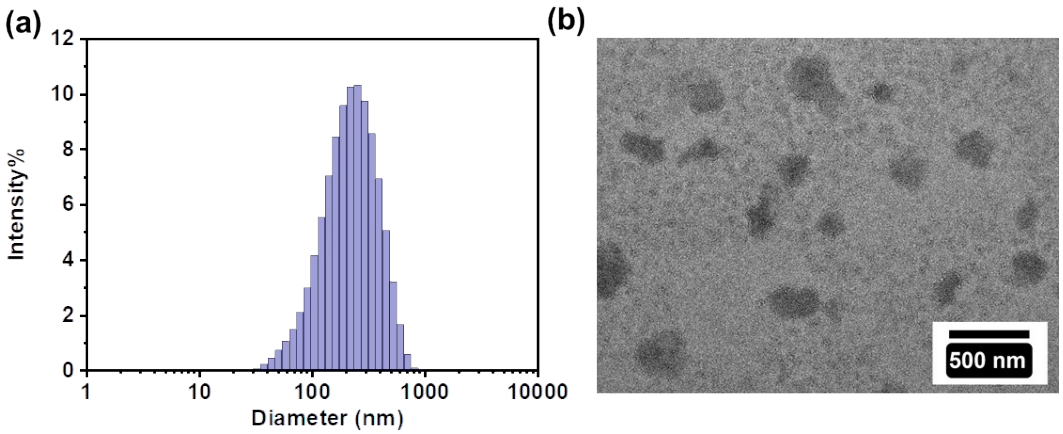

Figure S8. (a) The hydrodynamic diameter of **PyEn** in water determined by DLS. (b) TEM image of **PyEn**.

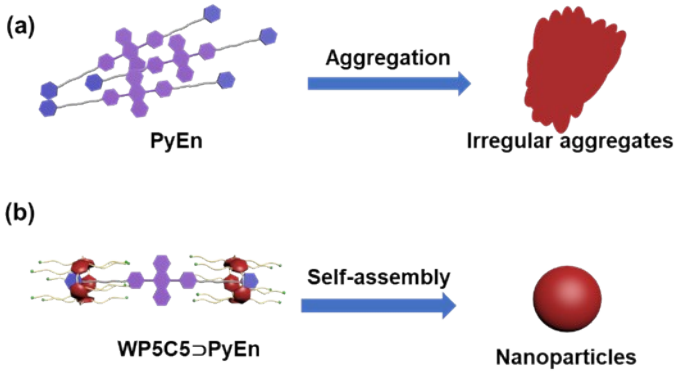

Figure S9. Cartoon representations of (a) aggregation of **PyEn** and (b) supramolecular self-assembly of **WP5C5⊃PyEn**.

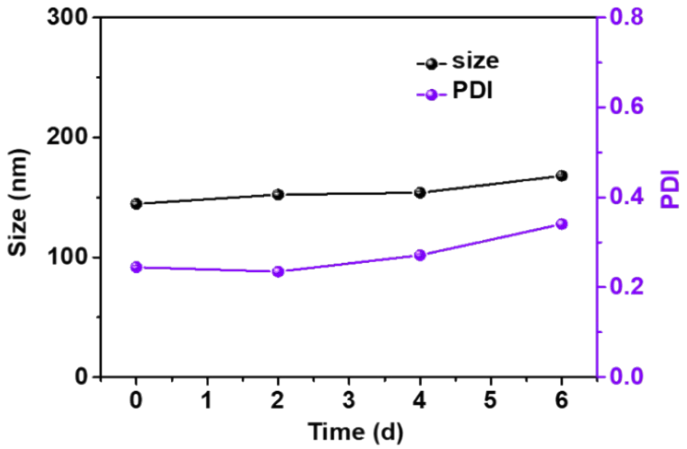

Figure S10. DLS measured hydrodynamic sizes and polydispersity index (PDI) of **WP5C5⊃PyEn** in water for 6 days.

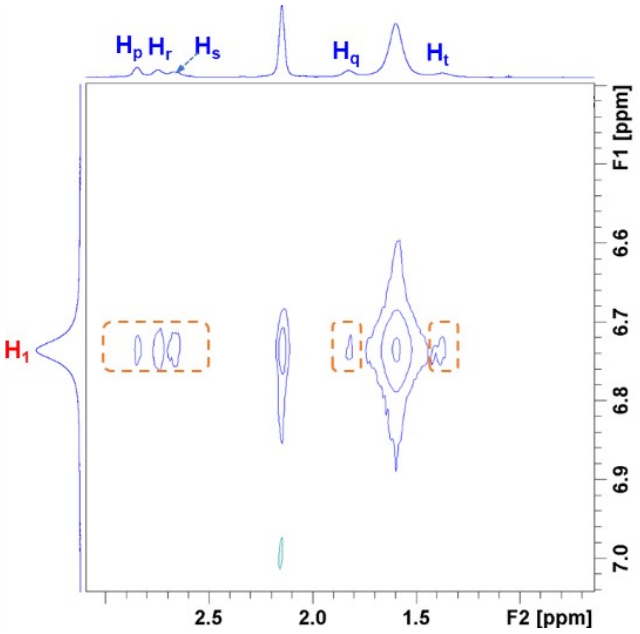

Figure S11. Partial 2D NOESY spectrum (600 MHz, D_2O, 298 K) of a mixture of **SPM** (5.0 mM) and **WP5C5** (5.0 mM).

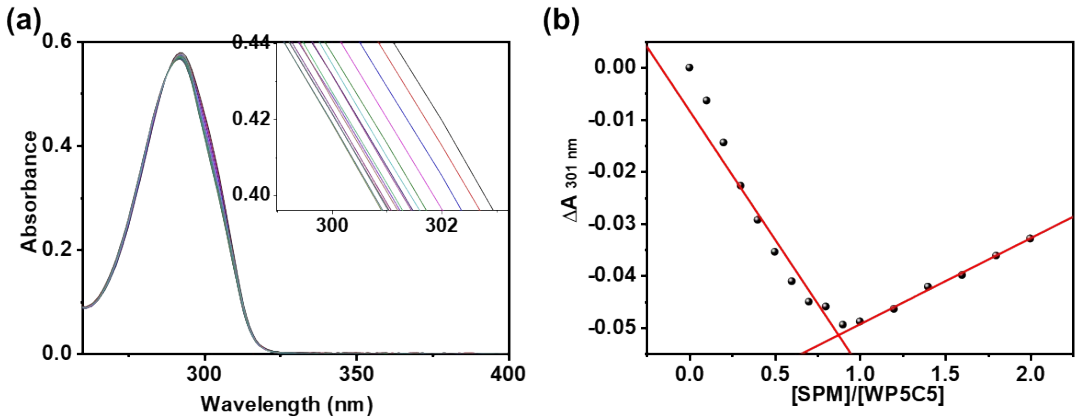

Figure S12. (a) UV-vis absorption spectra of the mixture of **WP5C5** and **SPM** in water at different molar ratio; (b) Plot showing the 1:1 stoichiometry of the complex between **WP5C5** and SPM by plotting the difference in absorption at 301 nm (a characteristic absorption peak of **WP5C5**) against the molar fraction of SPM at an invariant total concentration of 0.033 mM in aqueous solution.

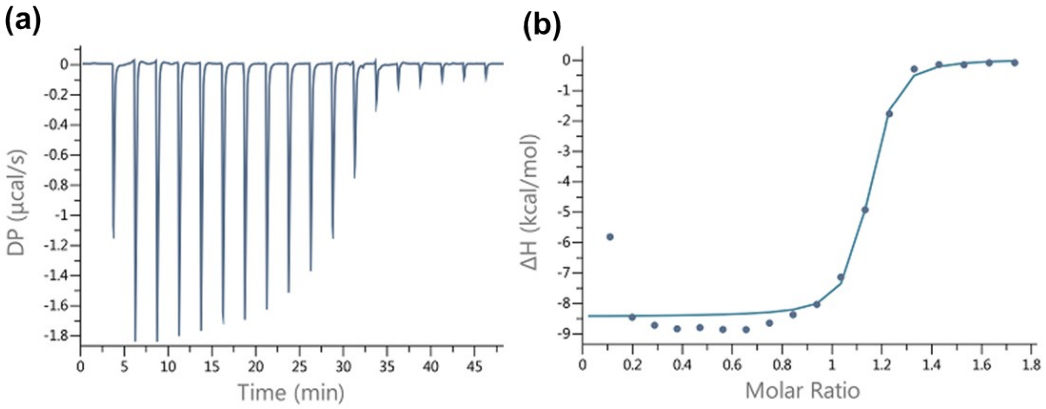

Figure S13. (a) Plot of DP *vs* time from the titration of host **WP5C5** (0.1 mM) and with guest SPM (1.00 mM) in H_2O; (b) plot of ΔH as a function of molar ratio. The solid line represents the best non-linear fit of the data to a 1:1 binding model (K_{app} = 5.32 × 10^6 M^{-1}, ΔH = -8.46 ± 0.52 kcal/mol, ΔG = -9.18 kcal/mol).

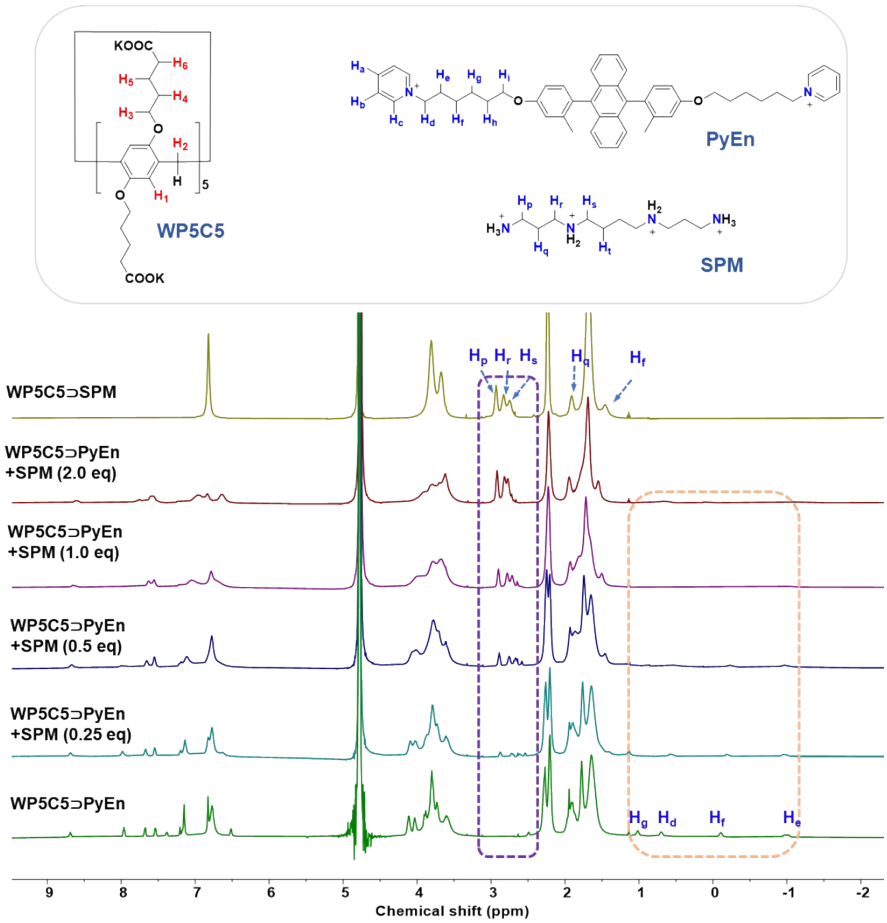

Figure S14. ^{1}H NMR spectra (600 MHz, D_2O, 298 K) of **WP5C5⊃PyEn** with the addition of increasing amount of SPM (0-2.0 equiv.).

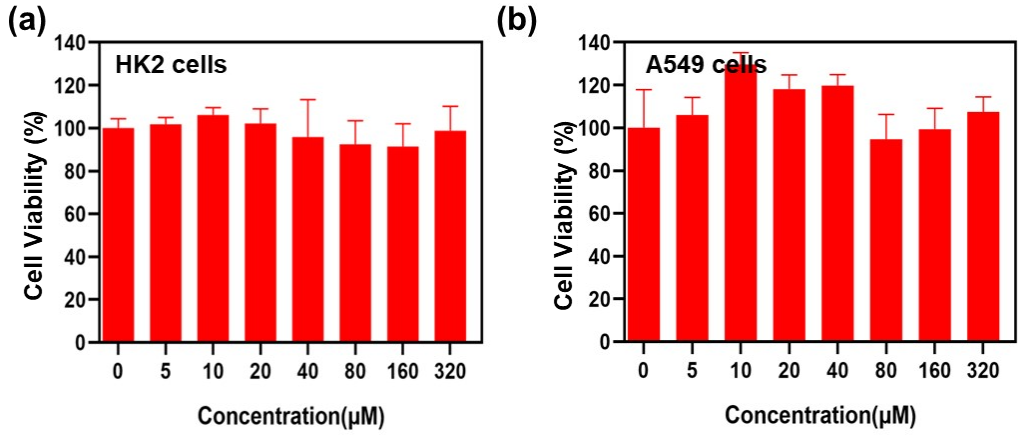

Figure S15. Cell viabilities of HK2 (a) and A549 (b) cells incubated with **WP5C5** for 24 h.

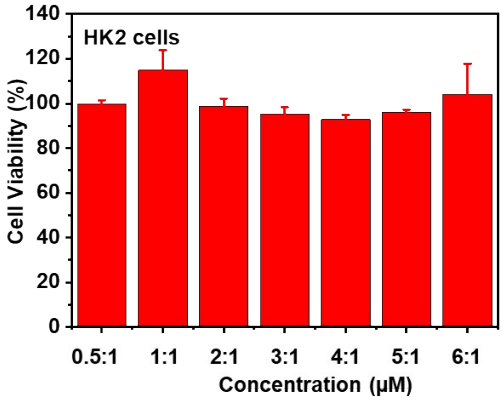

Figure S16. Cell viability of HK2 cells incubated with **WP5C5** and **PyEn** (10 μM) in different molar ratios for 24 h.

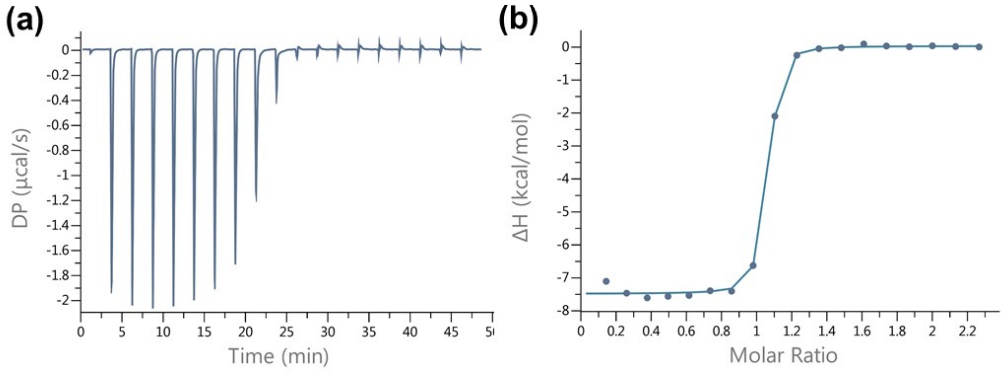

Figure S17. (a) Plot of DP vs time from the titration of host **WP5C2** (0.1 mM) and with guest **Gm** (1.00 mM) in H_2O; (b) plot of ΔH as a function of molar ratio. The solid line represents the best non-linear fit of the data to a 1:1 binding model (K_{app} = 1.35× 10^7 M^{-1}, ΔH = -7.51 ± 0.065 kcal/mol, ΔG = -9.73 kcal/mol).

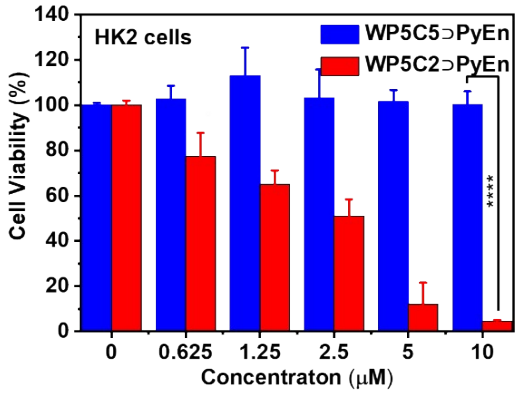

Figure S18. Cell viability of HK2 cells incubated with **WP5C5⊃PyEn** and **WP5C2⊃PyEn** for 24 h.

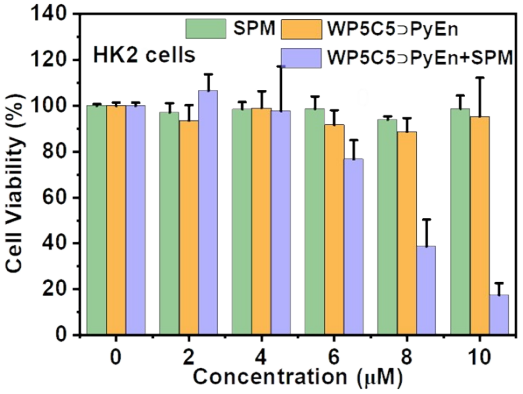

Figure S19. Cell viability of HK2 cells incubated with SPM, **WP5C5⊃PyEn**, and **WP5C5⊃PyEn**+SPM for 24 h.

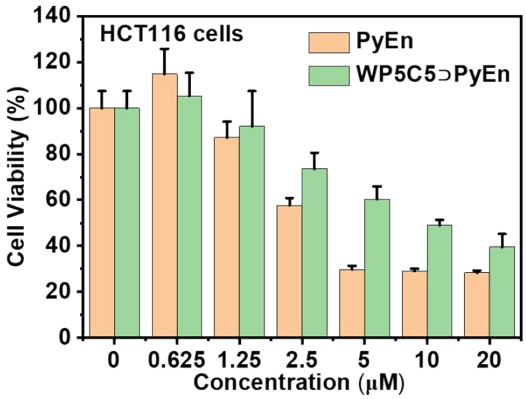

Figure S20. Cell viabilities of HCT116 cells incubated with **PyEn** and **WP5C5⊃PyEn** for 24 h.

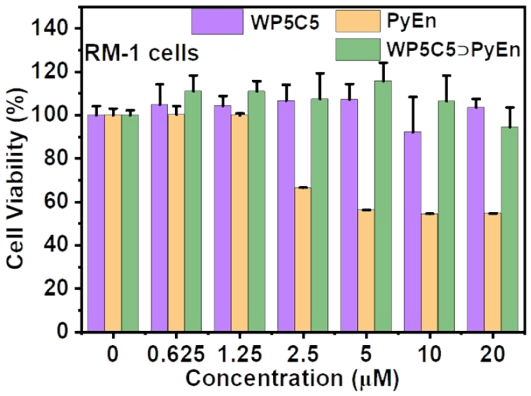

Figure S21. Cell viability of RM-1 cells incubated with **WP5C5**, **PyEn**, and **WP5C5⊃PyEn** for 24 h.

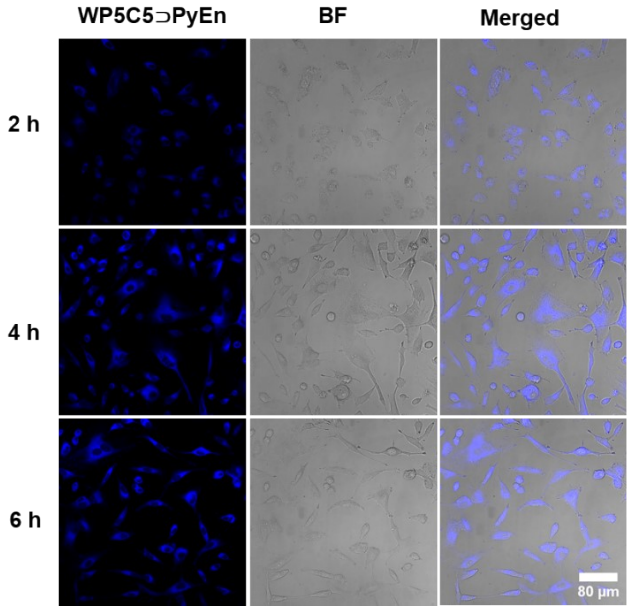

Figure S22. CLSM images of A549 cells treated with **WP5C5⊃PyEn** for 2 h, 4 h, and 6 h, respectively. Scale bars = 80 μm.

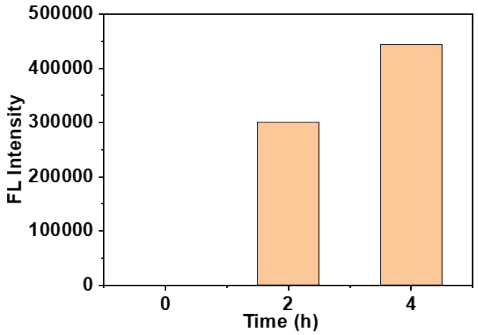

Figure S23. Flow cytometry analysis of A549 cells incubated with **WP5C5⊃PyEn** for 0 h (control), 2 h, and 4 h.

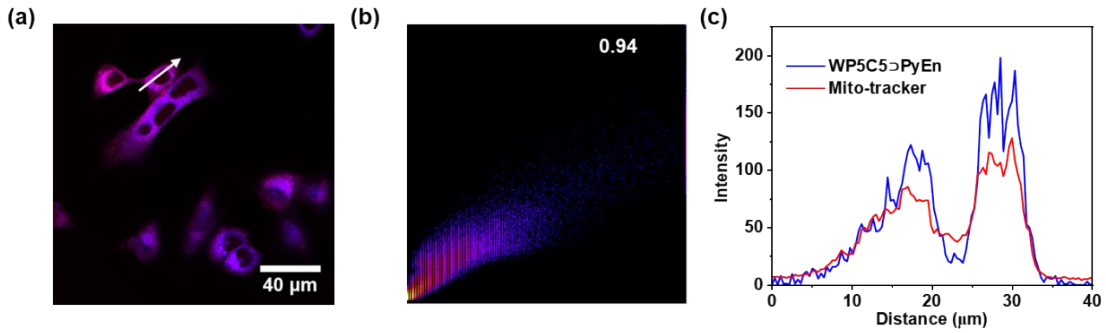

Figure S24. (a) CLSM images of A549 cells incubated with **WP5C5⊃PyEn** before being stained with commercialized Mito-tracker Red; (b) the scatter plot of Mito-tracker Red and **WP5C5⊃PyEn** across the cells; (c) Intensity profile within the regions of interest (ROIs; white line in (a)) of **WP5C5⊃PyEn** and Mito-tracker Red across the cells.

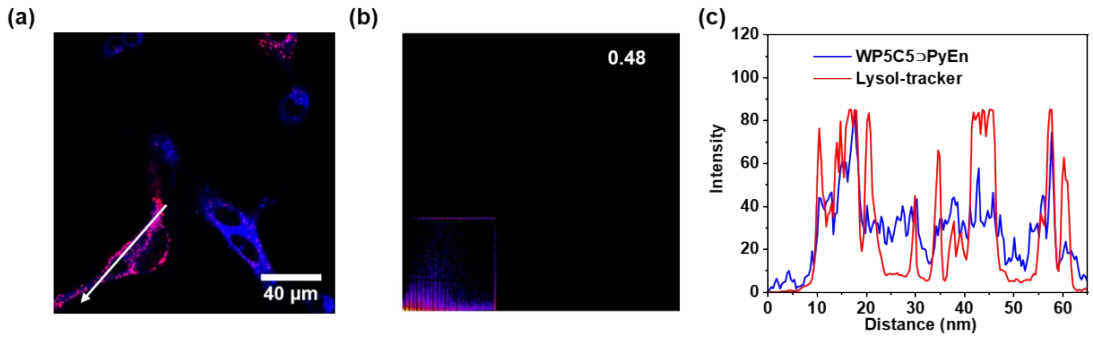

Figure S25. (a) CLSM images of A549 cells incubated with **WP5C5⊃PyEn** before being stained with commercialized Lysol-tracker Red; (b) the scatter plot of Lysol-tracker Red and **WP5C5⊃PyEn** across the cells; (c) Intensity profile within the regions of interest (ROIs; white line in (a)) of **WP5C5⊃PyEn** and Lysol-tracker Red across the cells.

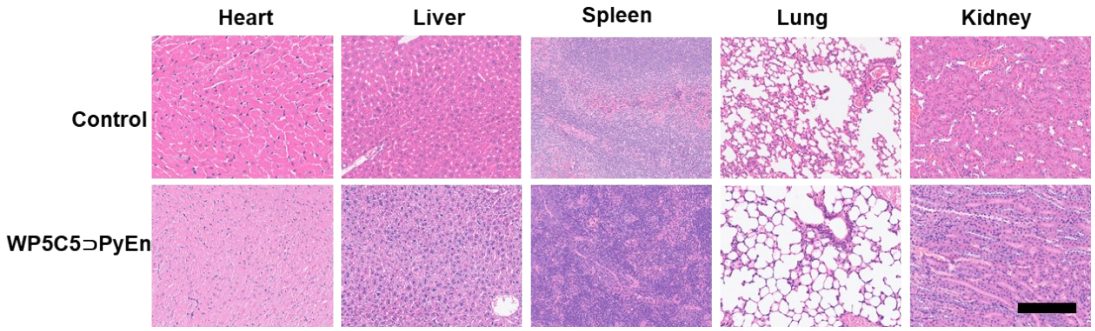

Figure S26. Images of various H&E-stained organ slices from A549/ADR tumor-bearing mice after different treatments on the 13th day after receiving the first treatment. Scale bar: 200 μm.

4. NMR (^{1}H and ^{13}C) and MS Spectra of New Compounds

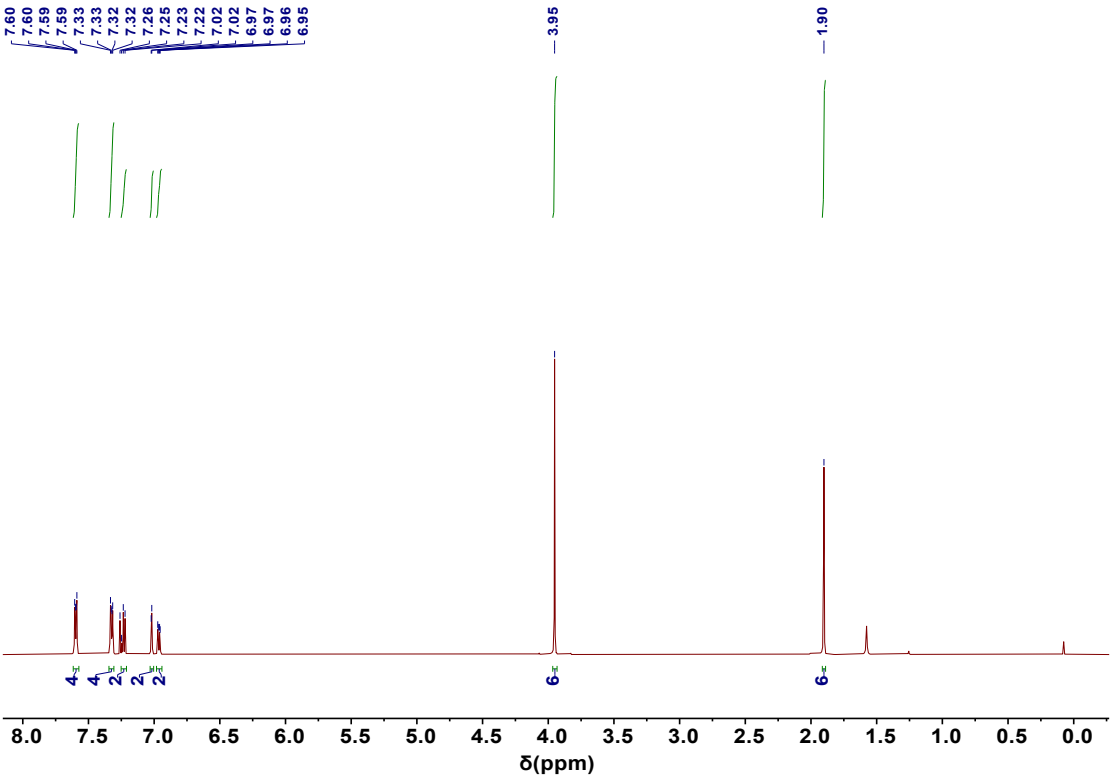

Figure S27. The ^{1}H NMR spectrum (600 MHz, 298 K) of compound **3** in $CDCl_3$.

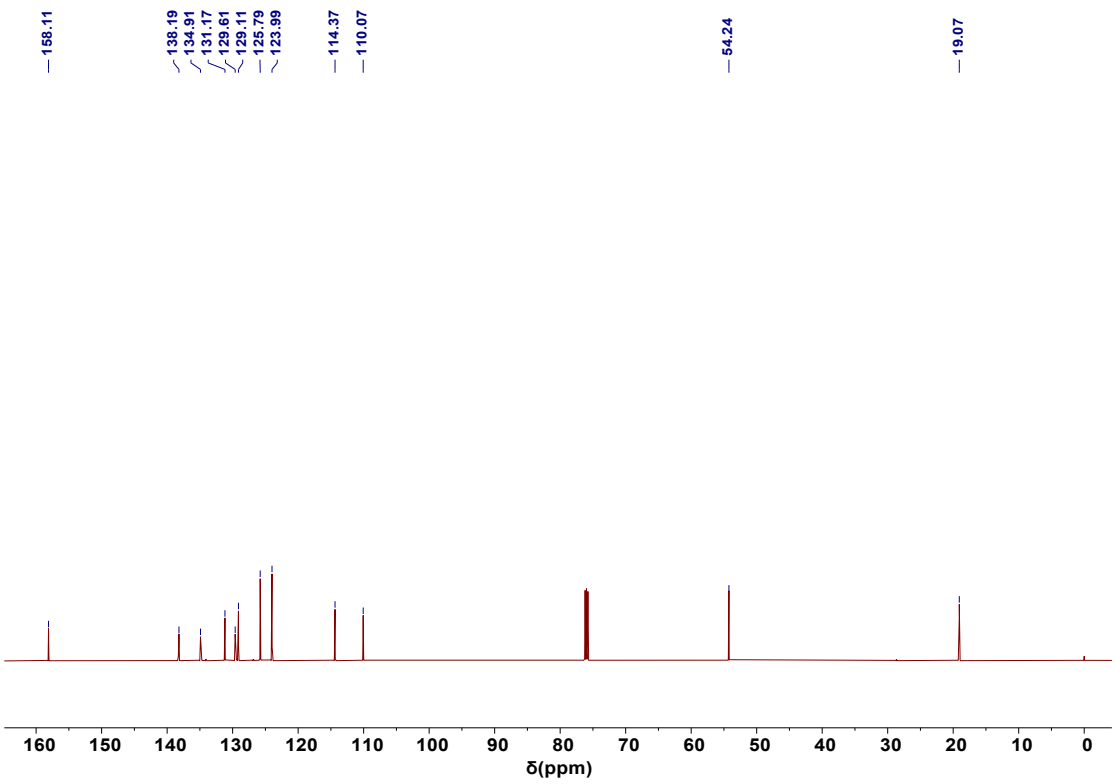

Figure S28. The ^{13}C NMR spectrum (150 MHz, 298 K) of compound **3** in $CDCl_3$.

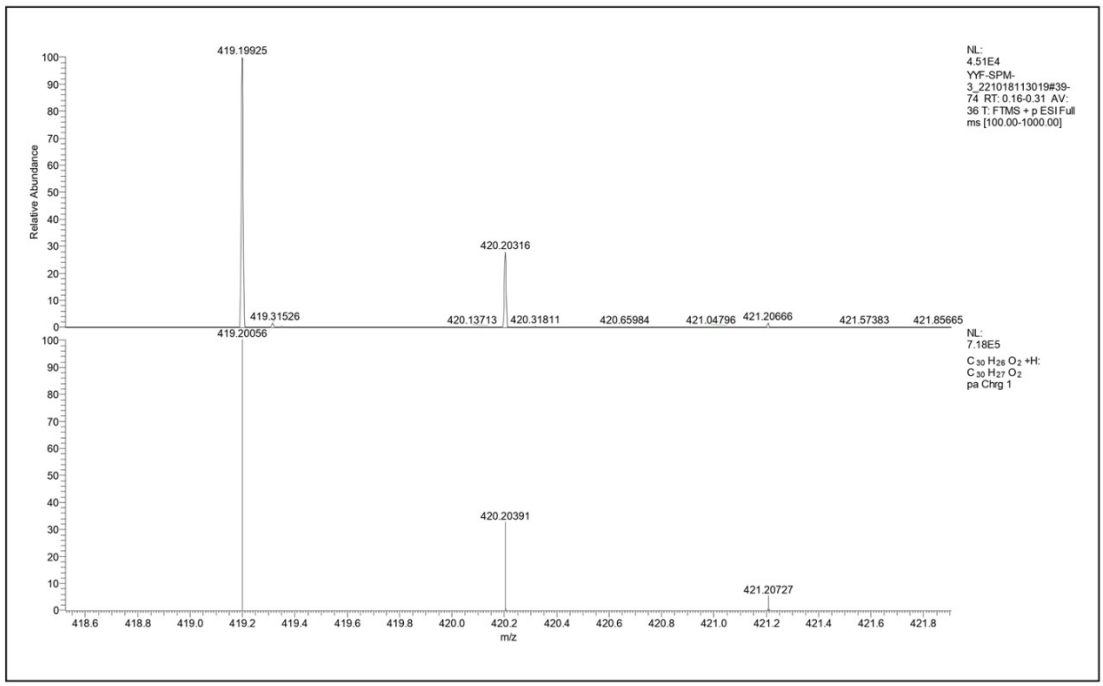

Figure S29. Mass spectrum of compound **3**.

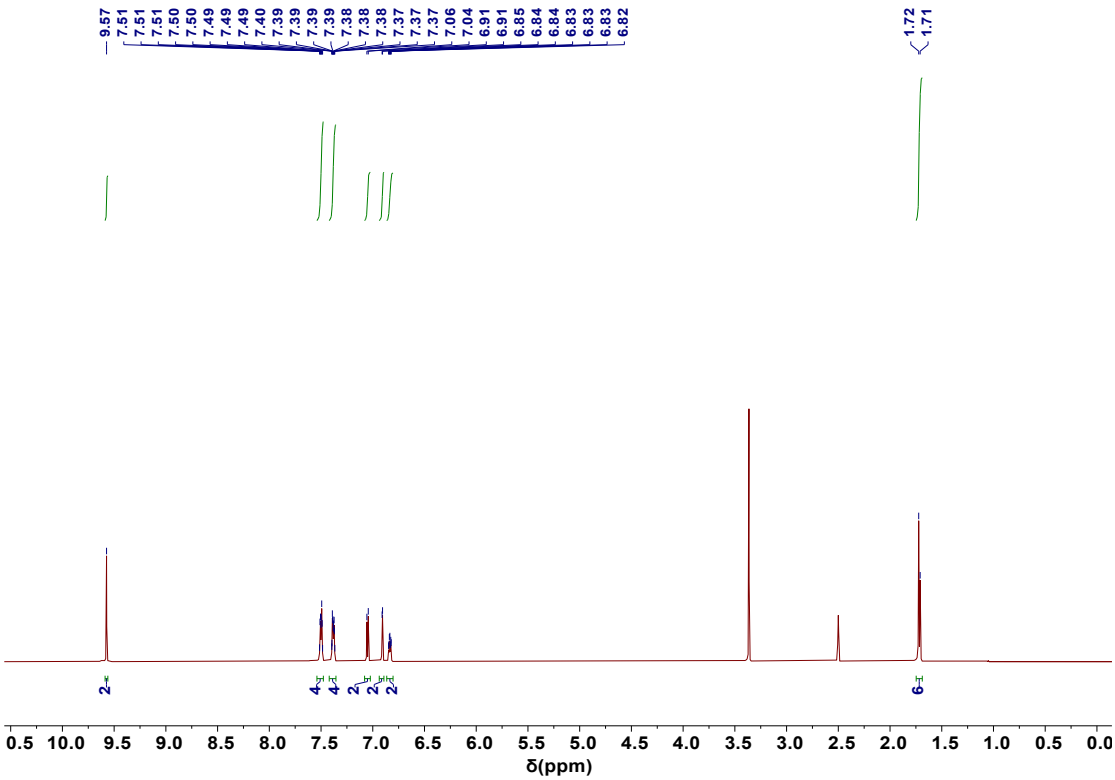

Figure S30. The ^{1}H NMR spectrum (600 MHz, 298 K) of compound **4** in DMSO-d_6

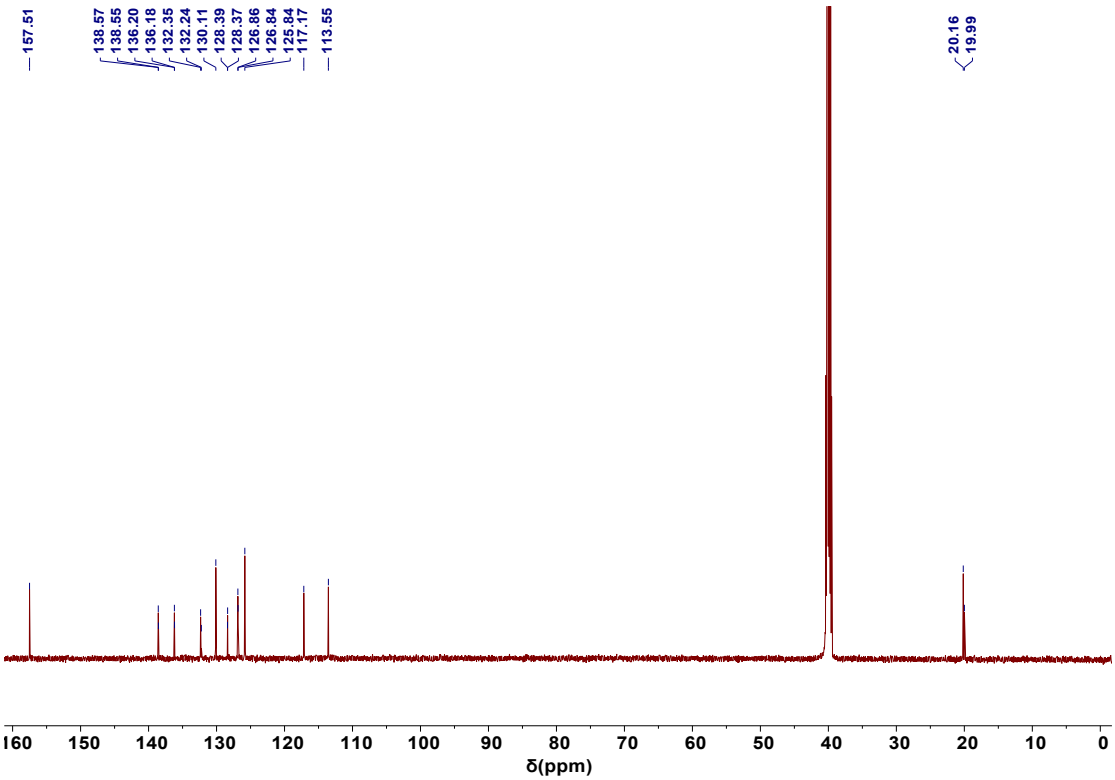

Figure S31. The ^{13}C NMR spectrum (150 MHz, 298K) of compound **4** in DMSO-d_6

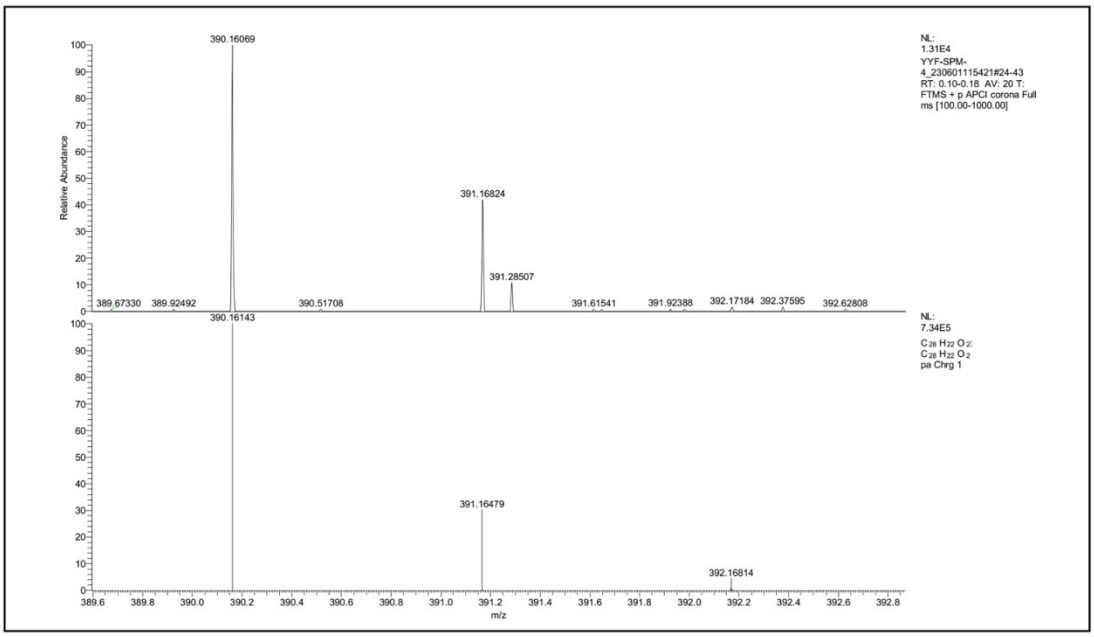

Figure S32. Mass spectrum of compound **4**.

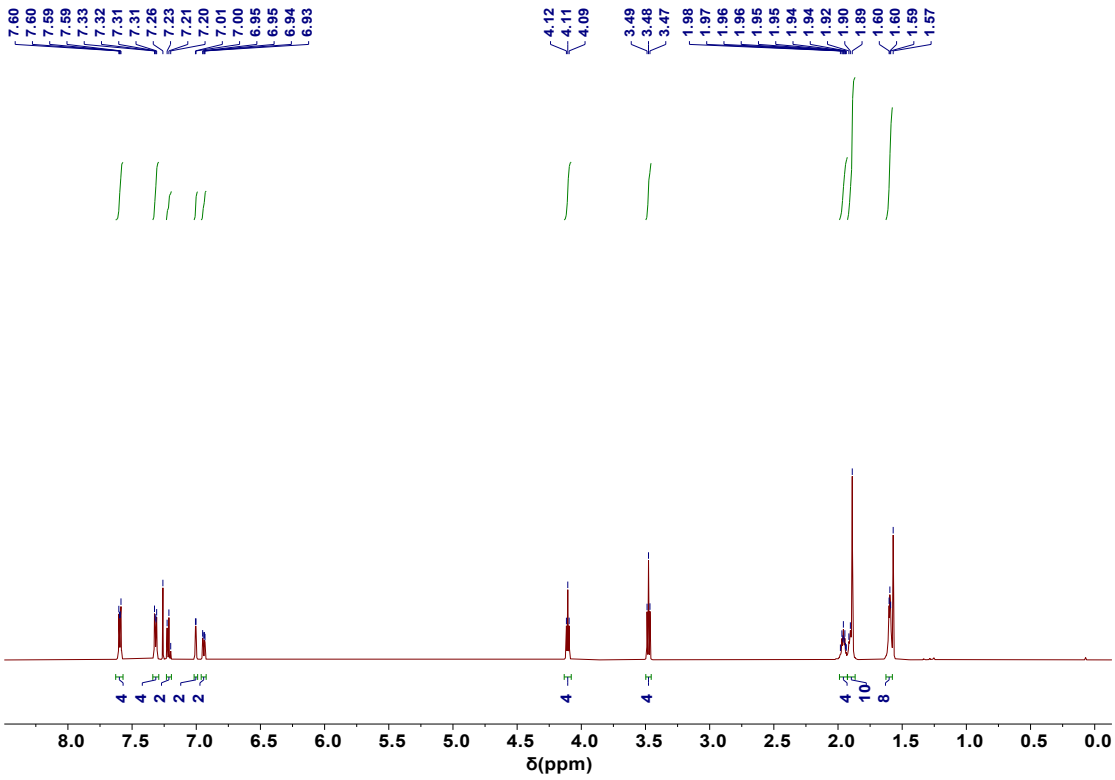

Figure S33. The ^{1}H NMR spectrum (600 MHz, 298 K) of compound **5** in $CDCl_3$.

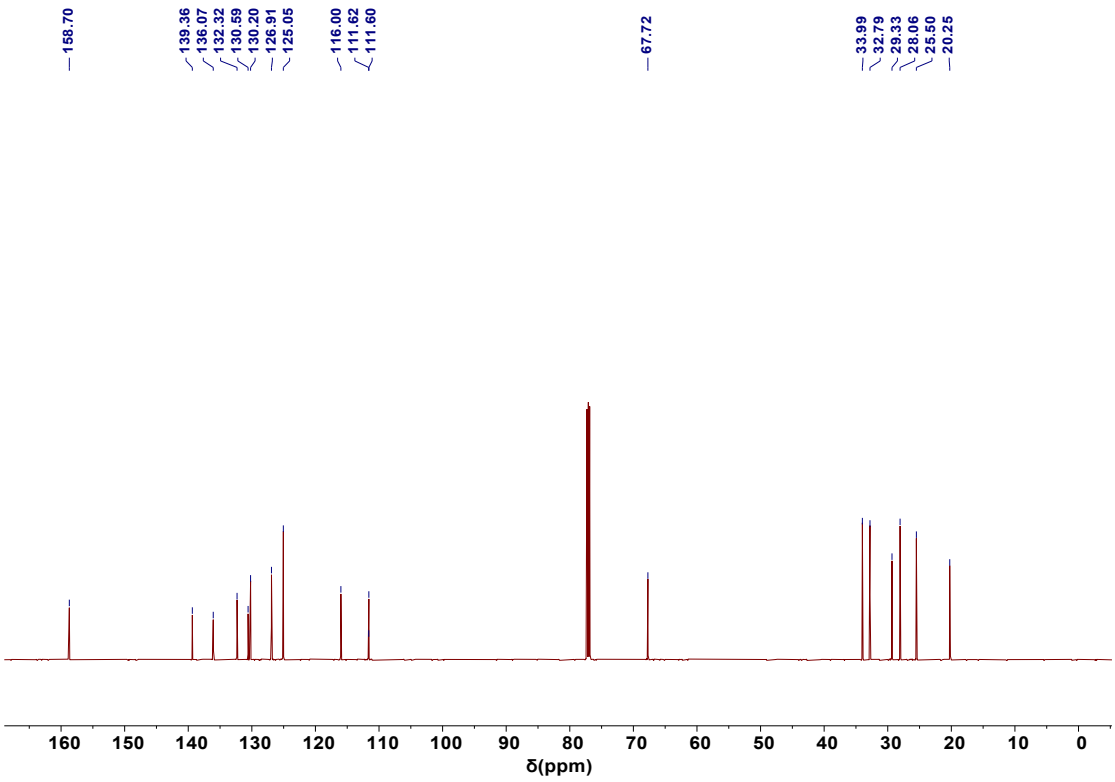

Figure S34. The ^{1}H NMR spectrum (150 MHz, 298 K) of compound **5** in $CDCl_3$.

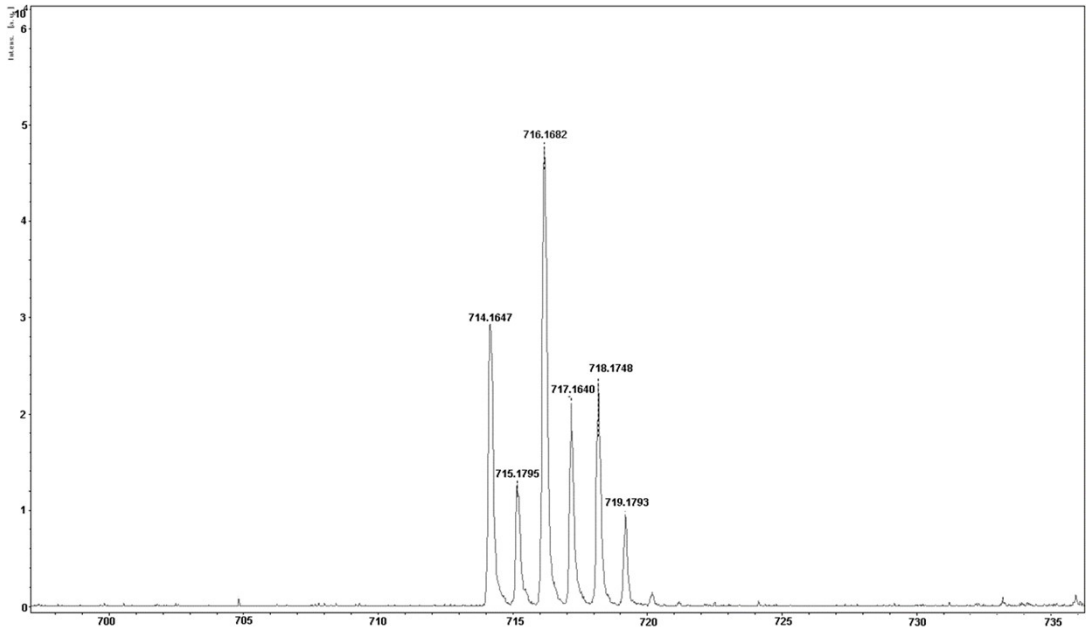

Figure S35. Mass spectrum of compound **5**.

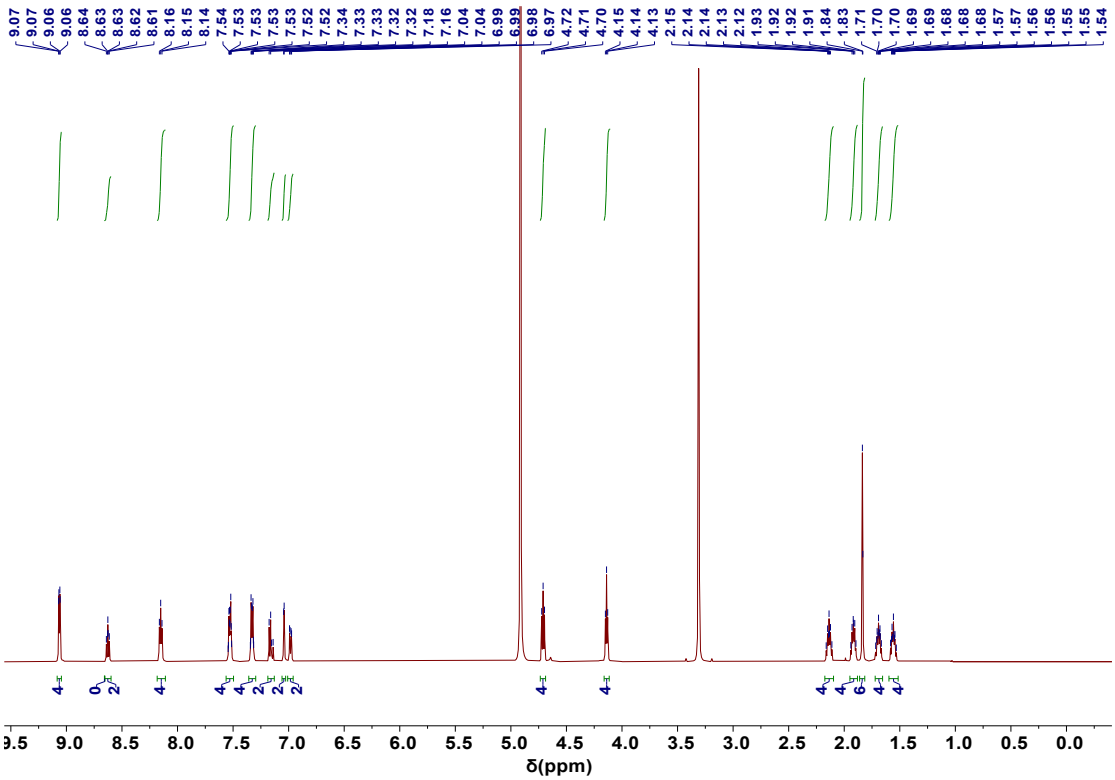

Figure S36. The ^{1}H NMR spectrum (150 MHz, 298 K) of compound **PyEn** in CD_3OD.

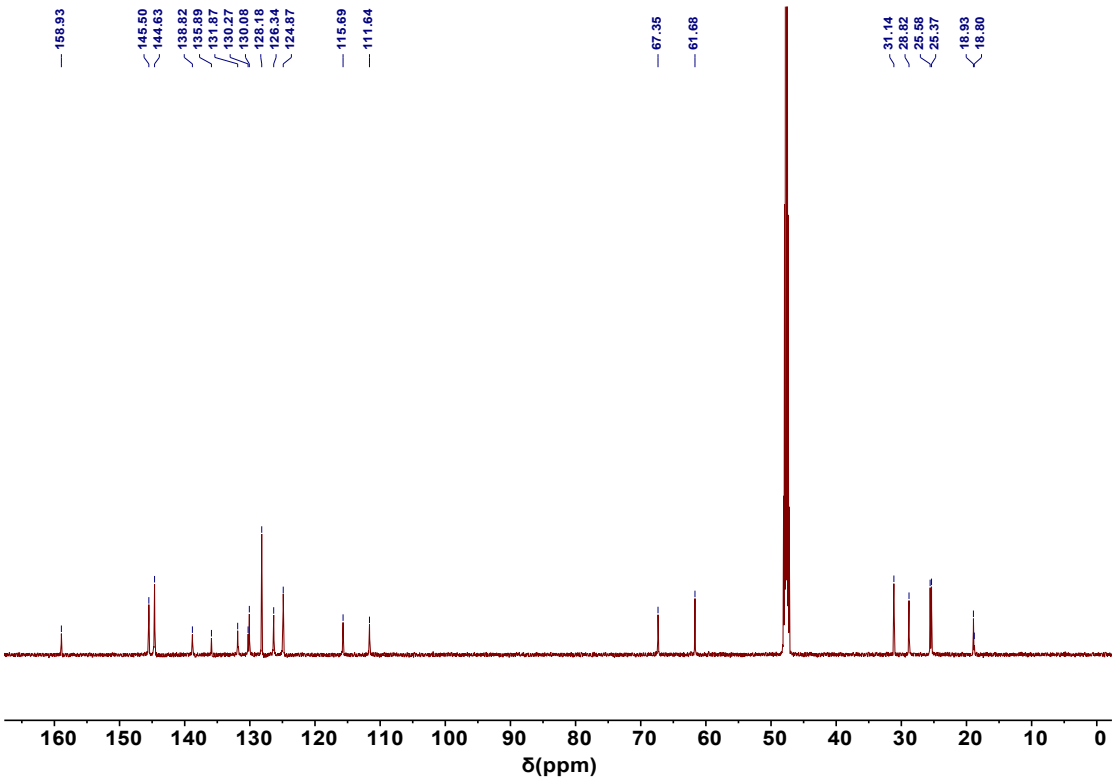

Figure S37. The ^{13}C NMR spectrum (150 MHz, 298 K) of compound **PyEn** in CD_3OD.

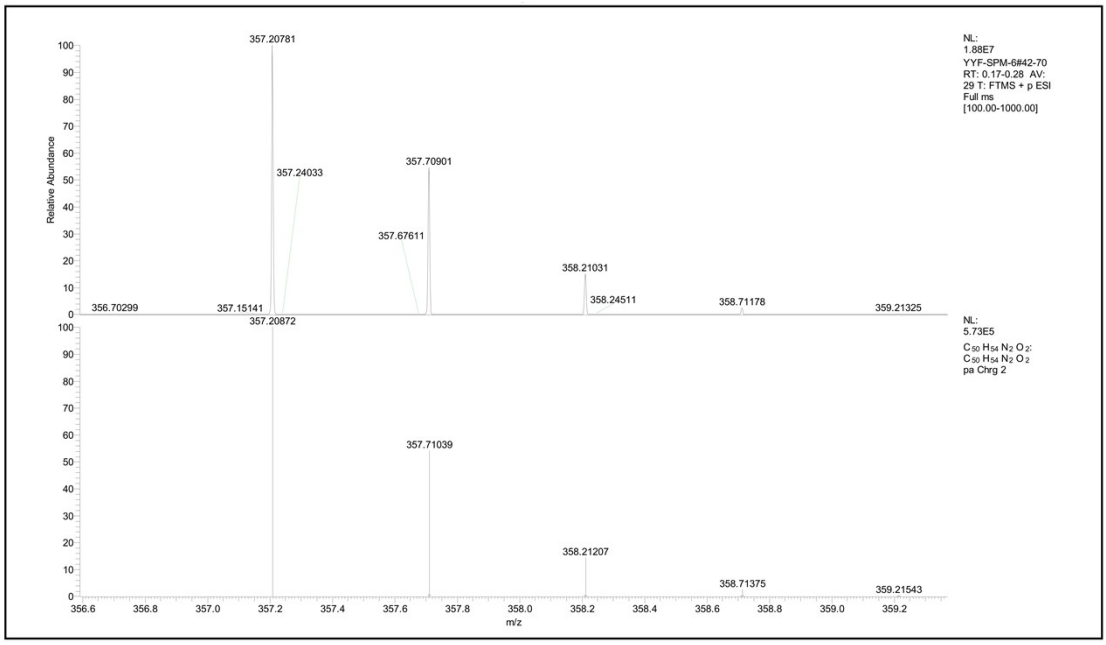

Figure S38. Mass spectrum of compound **PyEn**.

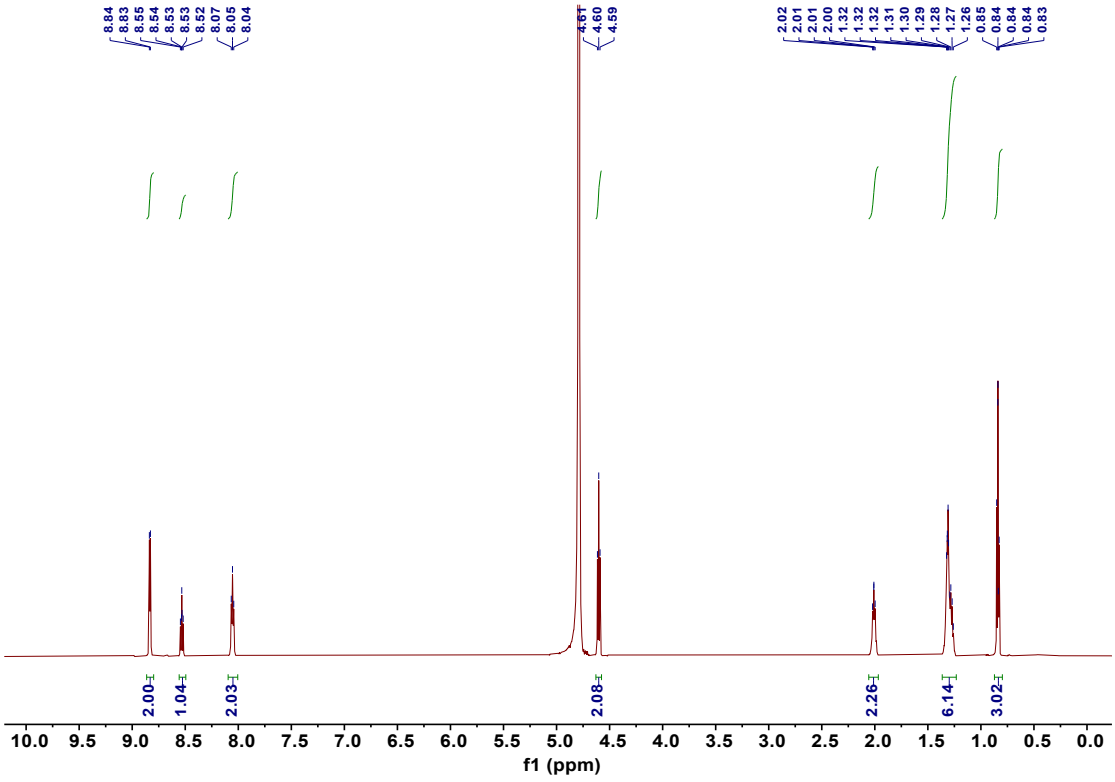

Figure S39. The ^{1}H NMR spectrum (600 MHz, 298 K) of compound **Gm** in D_2O.

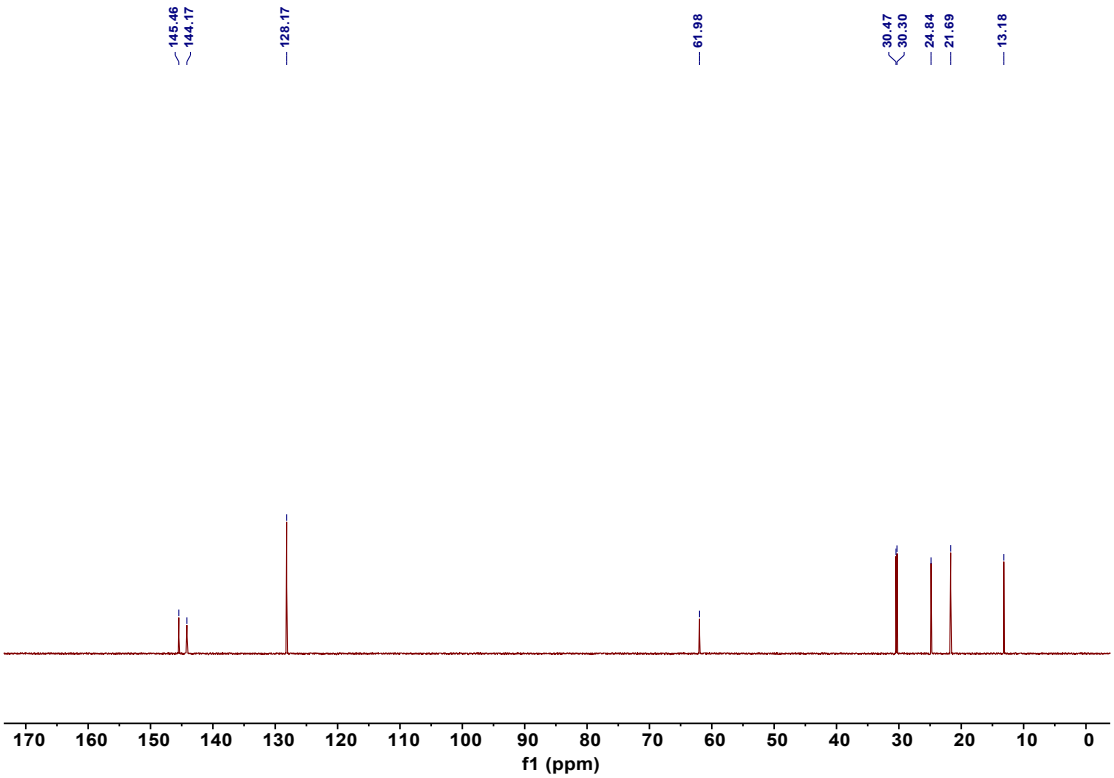

Figure S40. The ^{13}C NMR spectrum (150 MHz, 298 K) of compound **Gm** in D_2O.

5. References

1. Iken, H.; Guillen, F.; Chaumat, H.; Mazières, M.-R.; Plaquevent, J.-C.; Tzedakis, T., Scalable synthesis of ionic liquids: comparison of performances of microstructured and stirred batch reactors. *Tetrahedron Lett.* **2012,** *53* (27), 3474-3477.

2. Li, H.; Chen, D. X.; Sun, Y. L.; Zheng, Y. B.; Tan, L. L.; Weiss, P. S.; Yang, Y. W., Viologen-mediated assembly of and sensing with carboxylatopillar[5]arene-modified gold nanoparticles. *J. Am. Chem. Soc.* **2013,** *135* (4), 1570-6.

3. Li, X. B.; Zhou, S. Y.; Zhao, Q.; Chen, Y.; Qi, P.; Zhang, Y. K.; Wang, L.; Guo, C. L.; Chen, S. G., Supramolecular enhancement of charge transport through pillar[5]arene-based self-assembled monolayers. *Angew. Chem., Int. Ed.* **2023,** *62* (19), e202216987.